Formation of bound states in the continuum for a quantum dot with variable width

Evgeny Bulgakov[1,2] and Almas Sadreev[1]
[1]*Kirensky Institute of Physics, RU-660036, Krasnoyarsk, Russia*
[2]*Siberian State Aerospace University, Krasnoyarsk Rabochii, 31, Krasnoyarsk, Russia*
(Received 7 December 2010; revised manuscript received 28 February 2011; published 14 June 2011)

We consider mechanisms of formation of the bound states in the continuum in open rectangular quantum dots with variable width. Because of symmetry there might be bound states in the continuum (BSCs) embedded into one, two, and three continua because of the symmetry of system. These BSCs arise for selected values of the width. We show numerically that the BSCs can be excited for transmission of wave packets if the quantum dot width is varied in time and reaches these selected values of dot width. Moreover, we consider numerically a decay process of different eigenstates in the closed quantum dot to show that some of them trap in the BSC after the quantum dot is opened.

DOI: 10.1103/PhysRevB.83.235321 PACS number(s): 03.65.Nk, 05.60.Gg, 73.23.Ad, 73.21.La

I. INTRODUCTION

In 1929, von Neumann and Wigner[1] claimed that the single-particle Schrödinger equation could possess localized solutions that correspond to isolated discrete eigenvalues embedded in the continuum of positive energy states for some artificial oscillation bounded potential. Extension and some correction of this work was done by Stillinger and Herrick[2] who presented a few examples of spherically symmetric attractive local potentials with bound states embedded in the continuum (BSCs) of scattering states in the context of possible BSCs in atoms and molecules (e.g., Refs. 3–6). Friedrich and Wintgen[7] discussed the realization of BSCs in a hydrogen atom in a magnetic field. Afterward, it was suggested that BSCs might be found in certain two-electron systems.[2,8] Later in 1973 Herrik[9] and Stillinger[10] predicted a BSC in semiconductor heterostructure superlattices with specific choices of each layer in the superlattice in analogy with the von Neumann and Wigner oscillating potential.[1] This BSC was observed by Capasso *et al.* as a very narrow absorption peak.[11]

Examples of BSCs can be more easily found if one goes beyond the one-dimensional Schrödinger equation; for example, in model systems[12–20] or in real two-dimensional (2D) systems.[21–31] In the hard-wall approximation they are the solutions of the two-dimensional equation

$$-\nabla^2\psi(x,y) = (E\pi^2)\psi(x,y). \tag{1}$$

Here, E is measured in units of the characteristic electron energy $E_0 = \pi^2\hbar^2/(2md^2)$ with d being the width of the leads. A typical view of the open system is presented in Fig. 1. Note that the Helmholz equation (1) is applied not only for electron transmission through the quantum dot (QD) but also for microwave and acoustic transmission through billiards[32] and optical transmission in photonic crystals.[31,33] It is widely accepted that, below the well-defined threshold for the propagating states equal to 1, the eigenenergies of the Schrödinger equation are discrete and the corresponding eigenfunctions are square-integrable bound states. Above the threshold, the eigenenergies are distributed continuously and the corresponding eigenfunctions are extended. However, there might be bound states with discrete energies above the threshold (i.e., BSCs). Numerous considerations in model and real 2D open systems have demonstrated the BSC by a vanishing of the resonance width.[12–30]

The main feature of the BSC is that an incident wave passing through the QD has no coupling with the BSC; that is, the BSC can not be excited by this wave. We can say that the BSC is a "true dark state" as was proposed by Muraguchi *et al.*[34] Therefore, there is a question of excitement of the BSC by the incident wave. If even to transmit a wave packet (WP) through the scattering system the BSC cannot be excited. However, we can violate the orthogonality of the BSC to the scattering state by varying the QD's shape for transmission of the WP. We show numerically that this strategy is able to excite the BSC. Another strategy to achieve the BSC is to excite an eigenstate of the closed QD and open the QD afterward. However, before a study of these processes we consider mechanisms by which BSCs arise in open rectangular QDs.

II. MECHANISMS OF BOUND STATES IN CONTINUUM IN OPEN QUANTUM DOTS

The first, most obvious mechanism for the BSC is related to a symmetry of the system. Let us write the total Hamiltonian of the system of QD plus two leads (see Fig. 1) as follows:[35,36]

$$H = \sum_{C=L,R}\sum_{p_C}\int_{p_C^2}^{\infty} dE|E,C,p_C\rangle E\langle p_C,E,C| + \sum_b |b\rangle\epsilon_b\langle b| + \sum_{C=L,R}\sum_b\sum_{p_C}\int_{p_C^2}^{\infty} dE|b\rangle\, V_{bp_C}\langle p_C,E,C| + \text{H.c.}, \tag{2}$$

where the index b enumerates the eigenstates of the closed QD, the index $p_C = 1,2,3,\ldots$ does the continua (the channels of propagation) of the right and left lead, and V_{bp_C} are the coupling matrix elements between the eigenstates of closed QD and mode p_C of semi-infinite lead C. We consider that the leads are identical. Then the coupling matrix elements do not depend on the lead $C = L,R$ and are as follows:[35,36]

$$V_{bp} = \sqrt{\frac{1}{2\pi k_p}}\int_{-1/2}^{1/2} dy\,\sin[\pi p(y-1/2)]\frac{\partial\phi_b(0,y)}{\partial x}. \tag{3}$$

Here, $E = p^2 + k_p^2/\pi^2$, and k_p is the dimensionless wave number of channel p in units of the lead's width, $1/d$. We consider that the system is symmetric relative to an

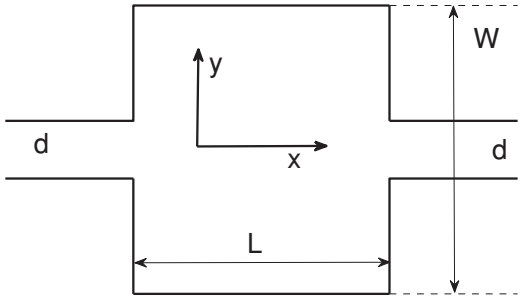

FIG. 1. Schematic view of rectangular QD with attached waveguides in hard-wall approximation.

inversion of the axis x, which is perpendicular to the transport axis x, as shown in Fig. 1. Then the eigenstates of the closed QD and the eigenmodes of the semi-infinite leads can be classified as even and odd states. In particular, the first, third, fifth, ... modes which define channels of the straight leads are even modes, while the second, fourth, ... modes are odd ones.

Let us consider the odd eigenstate ϕ_b of the closed QD with $\epsilon_b < 4$. Then the matrix element coupling that state with the first even-channel mode is $V_{b1} = 0$. Respectively, the state will not leak into the leads and could be defined as the BSC. However, the state ϕ_b is not eigen for the total Hamiltonian because of coupling with closed (evanescent) channels with $p = 3,5,\ldots$. As a result the last will slightly distort the odd eigenstate ϕ_b, transforming it into the BSC that is the eigenstate of the total Hamiltonian (2). We refer to the paper by Moiseyev[37] where an analysis of these BSCs based on symmetry arguments was presented.

The second mechanism of the BSC comes from a coupling of the eigenstate with the channel mode, which might go to zero upon varying the QD's width. For numerical purposes we take the model potential along the y axis in the following form:

$$V(y) = V_0\{1 + 0.5[\tanh[C(y - W/2)] - \tanh[C(y + W/2)]]\}, \quad (4)$$

which is shown in Fig. 2(a) where W is the effective width of the QD. This potential makes a QD with soft walls along the y axis. Let the eigenstate parity of the QD and the parity of the channel mode coincide so that $V_{b,p} \neq 0$. We start with the first even channel. For variation of the QD's width, the coupling matrix element might go to zero. It is clear that this might happen only for high eigenenergy to provide enough oscillations of the derivative $\frac{\partial\phi_b(0,y)}{\partial x}$ in the integral over y. Numerics shows that $V_{b,1}$ indeed goes to zero for $\epsilon_b > 4$.

Assume that, owing to the second mechanism, there is an odd BSC with the eigenenergy E_c uncoupled from the odd mode of the second-channel continuum at some fixed width W. Then, because of the parity of the first- and third-channel modes, this odd BSC is decoupled from the first- and third-channel continua. Therefore, by varying the QD's width, we can obtain a BSC embedded into two continua ($p = 1,2$) if $E_c < 9$ or even three continua ($p = 1,2,3$) if $E_C < 16$. We define these BSCs as second or third order, respectively. This contrasts with the quasibound states in a two-channel quantum wire that have been previously reported.[20]

The third mechanism of the BSC is the more sophisticated. Let each eigenstate of the QD be coupled with the continuum. Upon opening of the QD, they become resonances given by poles of the S-matrix in the complex energy plane. Then the BSC is the result of destructive interference of the resonances, which might be full with variation of the QD's width. That mechanism for the BSC was shown analytically in a two-level approximation for QDs coupled with one continuum[38–42] and was realized in two-dimensional systems. In particular, the third mechanism for the BSC has been realized in a quasi-one-dimensional constriction with an attractive, finite-size impurity by varying the size of the impurity,[21] in a bend waveguide for variation of bending,[22] and in an open QD for variation of the QD's width.[24] In Fig. 2(a) we present the pattern of a BSC with eigenenergy $E_c = 1.5845$ embedded into the continuum of the first channel, which is the result of the full destructive interference of two resonance states at $W = W_c = 2.7498, L = 4$. For the varying of the QD's width the conductance displayes avoided crossing of zero conductance with unit one.[24] This phenomenon was recently observed by Lepetit *et al.* in high-permettivity dielectric metamaterial resonator.[43]

Again, similar to the second mechanism, the BSC has zero coupling with the even first- and third-channel modes because of the destructive interference of odd-resonance states.

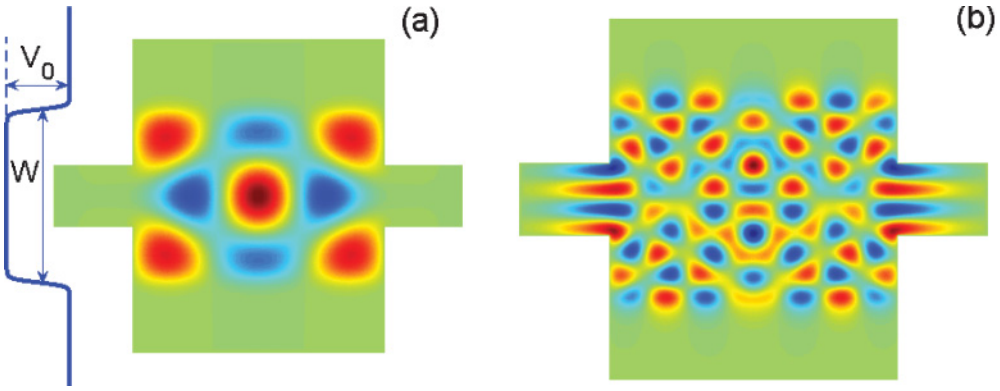

FIG. 2. (Color online) Patterns of BSCs with eigenenergy attributable to the third mechanism. (a) BSC with eigenenergy $E_c = 1.5845$ is the result of interference of two resonances that become full for the QD width $W = W_c = 2.7498, L = 4$. The width is governed by the soft potential (4), which squeezes the QD as schematically shown at left. (b) Extremely excited BSC with eigenenergy $E_c = 13.329$ embedded into three continua $p = 1,2,3$ for $W = 2.8731, L = 4$.

Therefore, such a BSC might be embedded simultaneously into the first-, second-, and third-continuum channels. We present in Fig. 2(b) a pattern of this extremely excited third-order BSC with eigenenergy $E_c = 13.329$. However, the most interesting thing is that this BSC is the result of full destructive interference of, at least, three resonance states. Thus, we report the numerical solution of the problem formulated by Miyamoto:[44] could the BSC exist because of the multilevel interference effect $b = 1,2,3,\ldots$ for $V_{b,p} \neq 0$?

The concept of a Fano mirror is the fourth mechanism for BSCs.[13,45,46] Let the closed system be composed of two identical scattering centers connected by a wire. If the transmission through each scattering center becomes zero, they can serve as ideal mirrors as in a Fabry-Perot interferometer. Then BSCs arise if an integer number of half waves are spaced between the Fano mirrors. This mechanism, exclusively transparent, was applied to a typical one-dimensional double-barrier structure with a periodically driven potential barrier,[45] to a photonic crystal structure with a waveguide coupled with two single-mode cavities,[13,46] and to two coupled identical quantum dots.[15,25,27,47–49]

Irrespective of the physical mechanism of the BSC, a general theory of BSCs can be formulated as follows: The scattering wave function in the interior of the QD obeys the Lippmann-Schwinger equation[36]

$$(H_{\text{eff}} - E)|\psi\rangle = \hat{V}|E,p\rangle, \tag{5}$$

where $|E,p\rangle$ is the state of channel p, and V is the coupling matrix given in Eq. (3). This formulation of the Lippmann-Schwinger equation implies that the wave is incident at channel p of the left lead and excites the state in the interior of the QD. The effective non-Hermitian Hamiltonian H_{eff} is the result of the Feshbach projection of the total Hamiltonian into the inner space of the closed QD:[35,36,42,50–52]

$$\langle b|H_{\text{eff}}|b'\rangle = \epsilon_b\delta_{bb'} + 2\sum_{p=1}^{\infty} V_{bp}\frac{1}{E^+ - H_p}V_{pb'}. \tag{6}$$

Here the factor 2 takes into account that the leads are identical. After some algebra the effective Hamiltonian takes the form[36,53]

$$\langle b|H_{\text{eff}}|b'\rangle = \epsilon_b\delta_{bb'} - 2\sum_{p=1}^{\infty} e^{ik_p}V_{bp}V_{b'p}. \tag{7}$$

The BSC that occurs for the inversion of matrix $H_{\text{eff}} - E$ does not exist [i.e., $\det(H_{\text{eff}} - E) = 0$].[18,24,31] That equation is a special case of the equation for the complex eigenvalues of the effective Hamiltonian

$$H_{\text{eff}}|\lambda) = z_\lambda|\lambda), \tag{8}$$

provided that one of the complex z_λ becomes real. Here, the complex eigenvalues $z_\lambda = E_\lambda - i\Gamma_\lambda/2$ where E_λ define the energy positions of resonances with resonance widths Γ_λ[51,52] if the resonance width is sufficiently small compared to the distance between resonances. The right eigenstates $|\lambda)$ with the left eigenstates $(\lambda|$ form the biorthogonal basis.[36,51]

Therefore, the condition for a BSC $\det(H_{\text{eff}} - E) = 0$ is equivalent to the often-used definition of a BSC as a resonance state $|\lambda)$ with vanishing width,[38,39,44,54] which is an eigenstate of the effective Hamiltonian

$$H_{\text{eff}}(E_c, W_c)|\text{BSC}\rangle = E_c|\text{BSC}\rangle. \tag{9}$$

$\langle\text{BSC}|V|E,p\rangle = 0$ for those channels p to which continuum the BSC is embedded. Comparison with Eq. (5) shows that the BSC is a homogeneous solution of the Lippmann-Schwinger equation. The solutions of Eq. (9) are shown in Fig. 2.

Let the energy be below the bottom of the second propagation band: $E < 4$ [i.e., $p = 1$ in Eq. (5)]. Then all k_p are imaginary except the first-channel wave number k_1. In particular, for the BSC energy we obtain $k_2 = 2.3926i$. Assume we can disregard all channels except the first because of the small value of $\exp(-|k_p|), p > 1$ and write the effective Hamiltonian as follows:[36,43]

$$\langle b|H_{\text{eff}}|b'\rangle = \epsilon_b\delta_{bb'} - 2e^{ik_1}V_{b1}V_{b'1}. \tag{10}$$

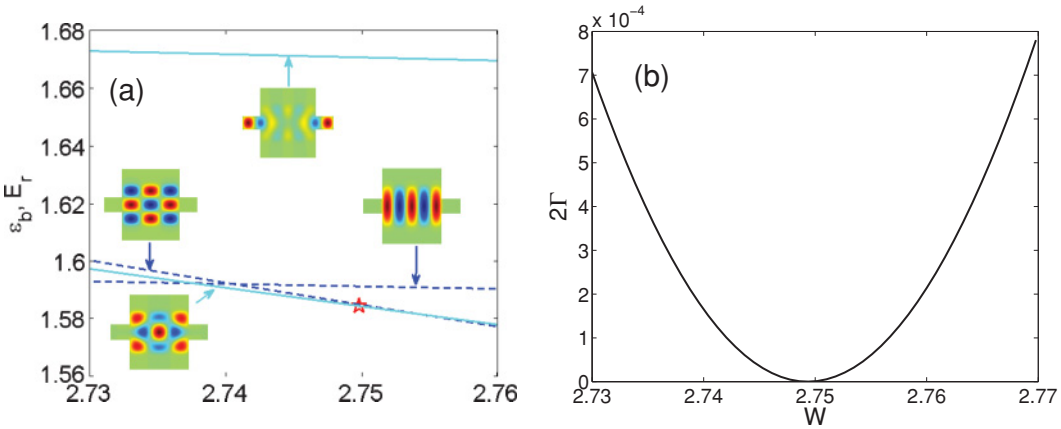

FIG. 3. (Color online) (a) Eigenfunctions ϕ_{33} and $\phi_{5,1}$ (in insets) and eigenenergies $\epsilon_{3,3}$ and $\epsilon_{5,1}$ of the closed QD versus the QD's width W are shown by dashed lines. The resonance energies E_r are shown by solid lines. The lower line is the resonance position whose width goes to zero at $W = W_c = 2.7498$, as shown in (b), and therefore gives rise to the BSC marked by the open star. The upper solid line corresponds to the superradiant solution[24,41] shown in inset. The corresponding resonance width with maximal width is not shown. Inset in bottom copies the BSC in Fig. 2.

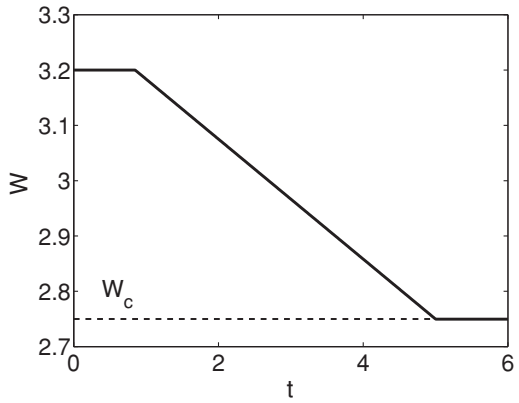

FIG. 4. Time evolution of the QD width (solid line). QD width starts with $W = 3.2$, then linearly decreases and reaches the width $W_c = 2.7498$ at which the BSC occurs.

For the effective Hamiltonian (10) the equation for the BSC takes the following form:

$$\det(H_{\text{eff}} - E) = \prod_b (E - \epsilon_b)\left(1 + 2e^{ik_1}\sum_b \frac{V_{b1}^2}{E - \epsilon_b}\right) = 0. \tag{11}$$

The equation is satisfied if the closed QD becomes degenerate (i.e., $\epsilon_b = \epsilon_{b'}$).[43] Mathematically, this result is based on the contribution of the continuum in the effective Hamiltonian being given by products of the matrix elements.

However, there is in fact an avoided crossing of the nearest resonance positions E_λ, as shown in Fig. 3(a) by solid lines. The first resonance width reaches zero at $W = W_c$ as shown in Fig. 3(b). Respectively, with correspondence to Eq. (9), the resonance state becomes a BSC as shown in bottom inset of Fig. 3(a). While the second resonance takes maximal width[38,39] [not shown in Fig. 3(b)] with the corresponding eigenstate (the superradiant state[41]) shown in Fig. 3(a) by the top inset. The BSC with eigenenergy $E_c = 1.5845$ is marked by the star in Fig. 3(a) and does not coincide with the crossing point of the nearest eigenenergies of the closed QD, shown by dashed

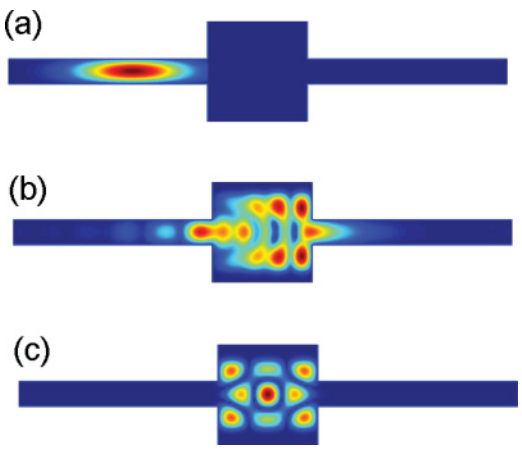

FIG. 5. (Color online) Snapshots of transmission of the wave packet by absolute value through the QD for the QD temporal squeezing shown in Fig. 4. Dark blue in snapshots corresponds to zero of wave function. (a) $t = 0$, (b) $t = 1$, and (c) $t = 5$.

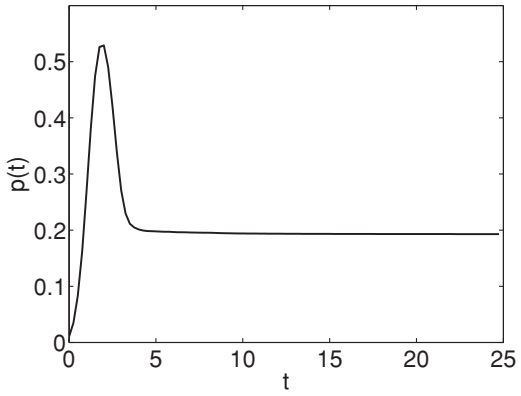

FIG. 6. Time evolution of the probability to be a quantum particle in the interior of QD for the wave-packet propagation shown in Fig. 5.

lines. The channels with $p > 1$ are the reason for this slight discrepancy. In fact, the effective Hamiltonian has the the following form:

$$\langle b|H_{\text{eff}}|b'\rangle = \epsilon_b\delta_{bb'} - 2e^{ik_1}V_{b1}V_{b'1} - 2\sum_{p=2}^{\infty} e^{-|k_p|}V_{bp}V_{b'p}, \tag{12}$$

for $E < 4$. Then the determinant of the matrix $(H_{\text{eff}} - E)$ cannot be rigorously reduced to Eq. (11), and equation (9) for the BSC can be solved only numerically with the results presented in Fig. 3. Numerics give that the BSC has energy $E_c = 1.5845$ and the resonance width goes to zero at $W = W_c = 2.7498$. These values at the BSC point are slightly different from the degeneracy point $W_d = 2.7405, \epsilon_d = 1.5921$. Thus, the evanescent modes of leads shift the BSC point from the degeneracy point. These results are in full agreement with the BSC occurring at those points where the resonance width goes to zero while the resonances undergo avoided crossings.[24,39] The effect of evanescent modes might be more profound for BSCs of higher eigenenergies, as shown later. In fact, even for the bound state with energy below the propagation band of closed channels, their contribution might be important.[55]

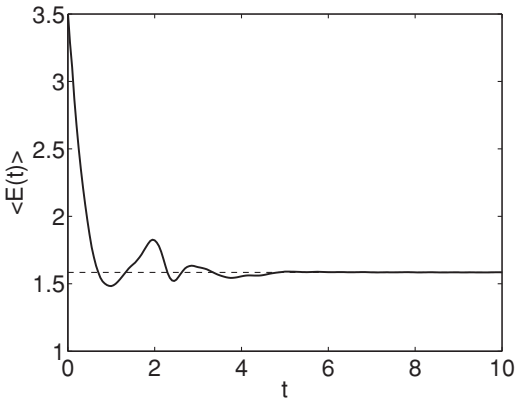

FIG. 7. Time evolution of the mean energy of the wave packet.

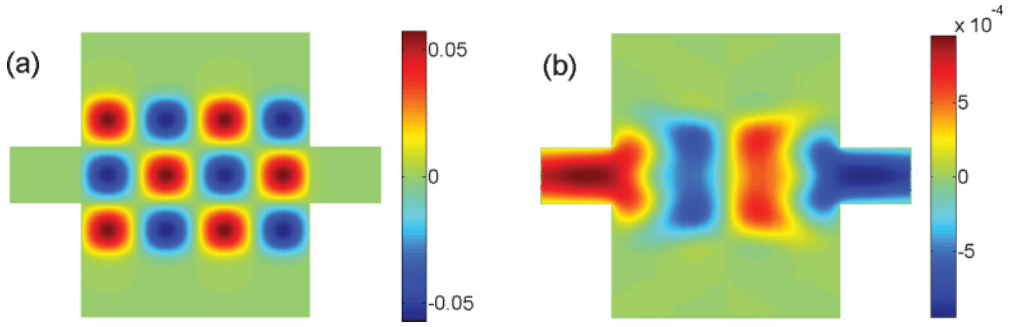

FIG. 8. (Color online) (a) Even eigenstate ϕ_{43} (a) with the eigenenergy $\epsilon_{43} = 1.9975$. (b) The state after $t = 100$. Sizes of the rectangular soft quantum dot are $L = 4, W_c = 2.7498$.

III. PROPAGATION OF WAVE PACKET THROUGH QUANTUM DOT WITH TIME-DEPENDENT SHAPE

The BSC is the square-integrable; that is, a localized eigenfunction of the total Hamiltonian (2) with the corresponding discrete eigenenergy embedded into the propagation band of scattering states. The BSC is orthogonal to other extended eigenstates of the total Hamiltonian, which are plane waves far from the scattering region presented by the QD under consideration. In other words, the BSC is "invisible" for waves transmited through the QD. Therefore, the BSC is orthogonal to the WP that is an expansion over the waves. For the propagating WP that could "see" the BSC, we violate temporarily this orthogonality for the transmission. One can apply a laser field of dipole type $e\vec{r} \cdot \vec{E}_0 \sin \omega t$ that breaks the parity of bound states and therefore mixes the bound state with the transport solution.[56] A similar approach was used recently by Muraguchi *et al.*[34] It was shown that, for transmission through the lozenge QD, the WP populates the even eigenstate of the QD that was transited into the odd bound state by absorbing a photon quantum. This last state has zero coupling with the first channel of leads and could therefore be the BSC if its energy were below 4. However, in Ref. 34 the energy of the stimulated odd bound state exceeded 4 to give rise to a decay into the second channel. In order to trap this state in the interior of the QD, sufficiently large potential barriers between the QD and leads were applied. That state was defined in Ref. 34 as a "quasi dark state."

We consider propagation of the WP through the symmetric rectangular QD and show that the BSC (true dark state) can be excited. In order to violate the orthogonality of the BSC to the WP we apply a slow time-dependent variation of the width of the QD. For that we apply the potential (4), which squeezes the QD's width W linearly in time as shown in Fig. 4. The parameters of the potential are the following: $V_0 = 10$, $C = 17$. For the QD, time dependence of the QD's shape can be easily achieved by an application of time-dependent gate voltage.

The final width of the billiard exactly corresponds to the BSC point shown in Fig. 3(a) by the star. For $t = 0$ the WP was taken as follows:

$$\psi_{\mathrm{WP}}(x,y,t=0) = \sin[\pi(y-1/2)] \exp[-(x+x_0)^2/(2\sigma^2) + ik_0 x], \quad (13)$$

with $x_0 = 5$, $\sigma = 1.5$, and $k_0 = 2.5$. It is located in the left input lead as shown in Fig. 5(a). In the next snapshots [Figs. 5(b) and 5(c)] one can see that, after the process of the WP transmission and the squeezing of the QD's width W, some part of the wave packet is trapped in the interior of the QD roughly after $t = 4$. Quantitatively, the process of trapping is shown in Fig. 6 as the time evolution of the probability to find the particle in the interior of the QD. Around time $t = 2$ the probability reaches a sharp maximum and afterward falls down and keeps constant for $t \geqslant 4$. The corresponding trapped wave function is shown in Fig. 5(c). Based on these figures we can conclude that these two processes of WP propagation and squeezing of the QD's width are able to excite the bound state with discrete energy within the first-channel continuum.

The BSC pattern shown in Fig. 2 is very close to the trapped wave function shown in Fig. 5 (c). Moreover, in Figure 7 we plotted the time evolution of the mean energy

$$\langle E(t) \rangle = \frac{\int_A dxdy \psi^*_{\mathrm{WP}}(x,y,t) H \psi_{\mathrm{WP}}(x,y,t)}{\int_A dxdy |\psi_{\mathrm{WP}}(x,y,t)|^2},$$

for the transmission of the wave packet through the QD. Here A is the area of the QD. The mean energy converges into the BSC eigenenergy $E_c = 1.5844$. Thus, these results unambiguously show that a part of the wave packet trapped in the QD is the BSC.

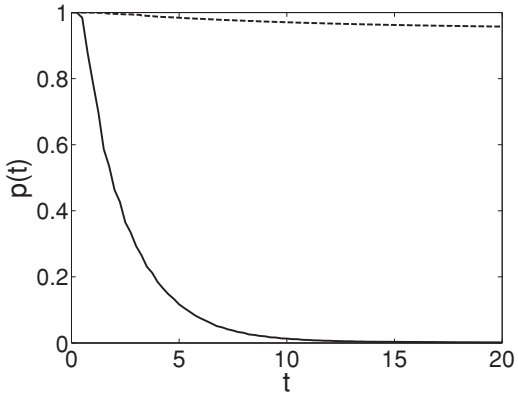

FIG. 9. Time evolution of the probability to find the quantum particle in the interior of the QD for the even initial state $\phi_{4,3}$ (solid line) and for the odd initial state $\phi_{3,4}$ (dashed line).

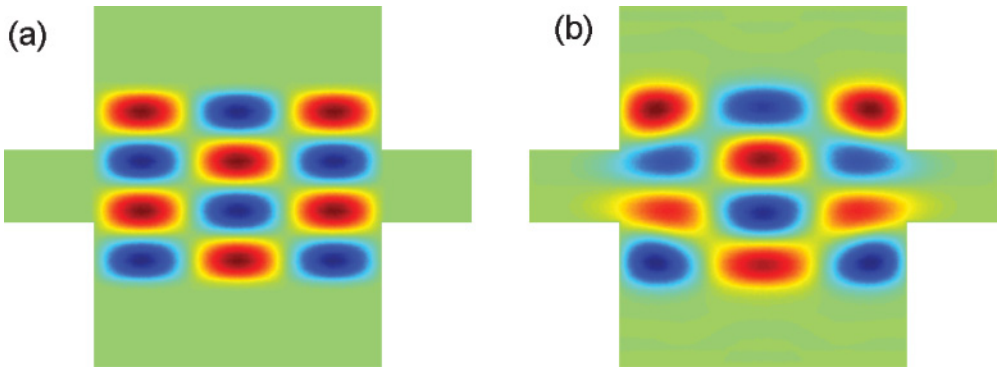

FIG. 10. (Color online) (a) Initial state is taken as the odd eigenstate $\phi_{3,4}$ with eigenenergy $\epsilon_{3,4} = 2.5735$. (b) Temporary state after $t = 100$ that is the BSC. QD sizes are the same as in Fig. 8.

IV. DECAY OF EIGENSTATES OF CLOSED QD AFTER OPENING

It is possible to achieve the BSC by decay of the eigenstates of the closed QD after opening an access to the attaching leads. The coupling can be governed by a voltage applied to the quantum point contact gates between the QD and electron waveguide. In microwave billiards the coupling can be varied via an electrooptic shutter as a diaphragm between the billiard and the waveguide.[32]

As given by Eq. (9), the BSC is the eigenstate of the effective non-Hermitian Hamiltonian. Therefore, it is reasonable to use the biorthogonal basis of the eigenstates of the effective Hamiltonian[35,36,51,57]

$$H_{\rm eff}|\lambda) = z_\lambda|\lambda), \quad (\lambda|H_{\rm eff} = z_\lambda(\lambda|, \quad z_\lambda = E_\lambda - i\Gamma_\lambda/2, \quad (\lambda|\lambda') = \delta_{\lambda,\lambda'}. \tag{14}$$

From the biorthogonality condition it follows that

$$\sum_\lambda |\lambda)(\lambda| = 1. \tag{15}$$

Moreover, by Hermitian conjugation of Eq. (14) we have

$$(\lambda|^* H^\dagger_{\rm eff} = z^*_\lambda(\lambda|^*. \tag{16}$$

These conjugated eigenstates form a biorthogonal basis, too.

Then, for the probability, we have to find the particle in the interior of the QD:

$$p(t) = \langle\psi_{\rm B}(t)|\psi_{\rm B}(t)\rangle = \sum_{\lambda,\lambda'}\langle\psi_{\rm B}(0)|\lambda^*)(\lambda^*|\exp(iH^\dagger_{\rm eff}t) \times \exp(-iH_{\rm eff}t)|\lambda')(\lambda'|\psi_{\rm B}(0)\rangle = \sum_{\lambda,\lambda'}\langle\psi_{\rm B}(0)|\lambda^*)(\lambda^*|\lambda') \times \exp[i(E_\lambda - E_{\lambda'})t - (\Gamma_\lambda + \Gamma_{\lambda'})t](\lambda'|\psi_{\rm B}(0)\rangle. \tag{17}$$

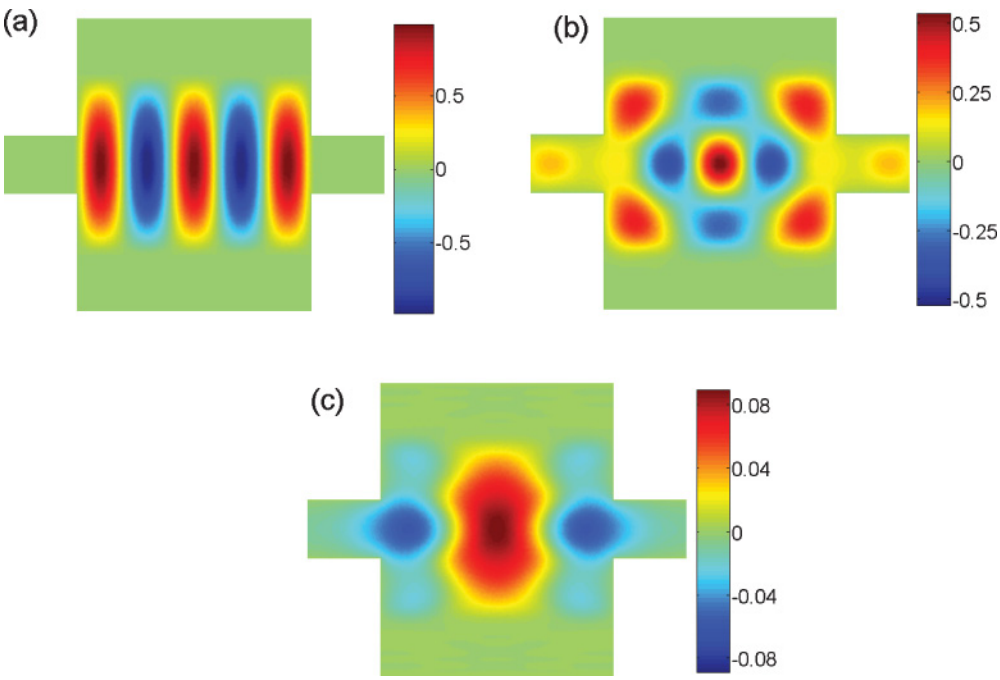

FIG. 11. (Color online) (a) Even eigenstate ϕ_{51} with the eigenenergy $\epsilon_{51} = 1.59$ for $W = 3$. (b) That state fast decays into the quasi BSC close to the exact BSC shown in Fig. 2 after $t = 1$. (c) After this, the quasi BSC decays over a long time and evolves into the truly bound state below the propagation band of the first channel after $t = 100$.

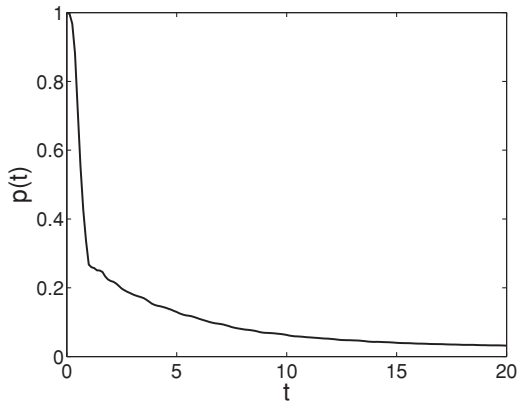

FIG. 12. Time evolution of the probability to find a quantum particle in the interior of the QD for the initial state $\phi_{5,1}$ and eigenenergy $\epsilon_{5,1} = 1.59$. The parameters of the QD are $W = 3$, $L = 4$.

where a subscript "B" means the state projected into the interior of the QD. Therefore, for the limit $t \to \infty$ we obtain that only the state with $\Gamma_\lambda = 0$ will survive in the interior of the QD. This result is in full correspondence with the definition of the BSC given by Eq. (9).

At first, we consider the decay of the even eigenstate ϕ_b of the closed QD with the eigenenergy $\epsilon_b < 4$. The eigenstates of the closed QD with soft walls along the y axis are

$$\phi_{m,n}(x,y) = \sqrt{\frac{2}{L}} \sin\left(\frac{m\pi(x - L/2)}{L}\right) \phi_n(y; W). \quad (18)$$

We assume that, for the initial time, the pure state $\psi_{m,n}$ with odd integer n is populated, and after an access into the leads is arisen. We can expect the probability to decay because of leakage into the leads with the characteristic decay time $\tau_{b,1} = \frac{1}{\Gamma_{b,1}}$ with $\Gamma_{b,1} = 2\pi|V_{b1}|^2$.[35] The factor 2 in the decay time is because two identical leads are attached to the QD. The subscript "1" means the first-channel mode of the leads.

Let us take, for example, the even eigenfunction as $b = (4,3)$ with the corresponding eigenenergy $\epsilon_{4,3} = 1.9975$ for $W = W_c = 2.7498, L = 4$. We evaluated the resonance width $\Gamma_{b1} \approx 0.22$ in units of $E_0/\hbar$ where we used Eq. (3) to obtain $k_1 \approx \pi\sqrt{\epsilon_b - 1}$. The initial state $\phi_{4,3}$ evolves after long time $t = 100$ into the state shown in Fig. 8(b) that is close to the eigenstate $\phi_{4,1}$. However, because of evanescent modes of the waveguides it blows up into the bound state below the propagation band of the first channel, as seen from Fig. 8(b). The corresponding probability $p(t) = \int_A |\psi(x,y,t)|^2 dxdy$ to find a quantum particle in the interior of the QD has typical exponential behavior $p(t) \approx e^{-\Gamma_{b1}t}$, as shown in Fig. 9. This result allows us to evaluate $\Gamma_{b1} \approx 0.223$, which agrees with the earlier evaluated result for Γ_{b1}.

Next, we consider the odd eigenstate $\phi_{3,4}$ that has zero coupling with the first-channel mode of leads: $\Gamma_{b,1} = 0$. Therefore, the particle in this state will not leak into the leads. In other words, the odd eigenstates of the closed QD with the eigenenergies below 4 are expected to be the BSCs. In fact, they are not truly the eigenstates of the total Hamiltonian (2) because of their coupling with the next evanescent modes of the leads with $p > 1$. As a result, the initial state $\psi(0) = \phi_{3,4}$ will slightly blow up from the QD and distort as shown in Figs. 10(a) and 10(b) to finally transfer into the true BSC. The corresponding time evolution of the probability is shown in Fig. 9 by the dashed line.

As for the third initial state, we take the eigenstate $\phi_{5,1}$, the parity of which coincides with the parity of the first-channel continuum. We take the width $W = 3$ close to the BSC point $W_c = 2.7405$. The eigenenergy $\epsilon_{5,1} = 1.59$ for $W = 3$ is slightly above the BSC energy $E_c = 1.5844$. Therefore, for an expansion of $\phi_{5,1}$ over the eigenstates of the effective Hamiltonian we may expect that the contribution of that eigenstate $|\lambda_c(W))$ is important, which transfers into the BSC for $W \to W_c$. Indeed, the snapshot in Fig. 11(b) reveal a fast recovery of the state close to the BSC shown in Fig. 2. Nevertheless, the state $|\lambda_c(W))$ is not the true BSC for $W \neq W_c$ and has therefore small but finite $\Gamma_\lambda(W)$. Then, in correspondence with Eq. (17), we have a slow decay of that state into some truly bound state with energy below the propagation band, as shown in Fig. 11(c). Indeed, the time evolution of the probability to find a particle in the interior of the QD reveals two decay times, as Fig. 12 shows.

Finally, we consider the decay of the highly excited eigenstates whose eigenenergies are embedded into the propagation band of the second- and third-continuum channels. In order for the soft potential $V(y)$ to confine the particle, we take $V_0 = 10$ if $\epsilon_b < 9$ and $V_0 = 25$ if $9 < \epsilon_b < 16$. Let us take, first, the even eigenstate $\phi_{6,7}$ with the eigenenergy $\epsilon_{6,7} = 6.9253$ that is below the third-channel propagation band. The state is uncoupled with the second channel, but is coupled with the first

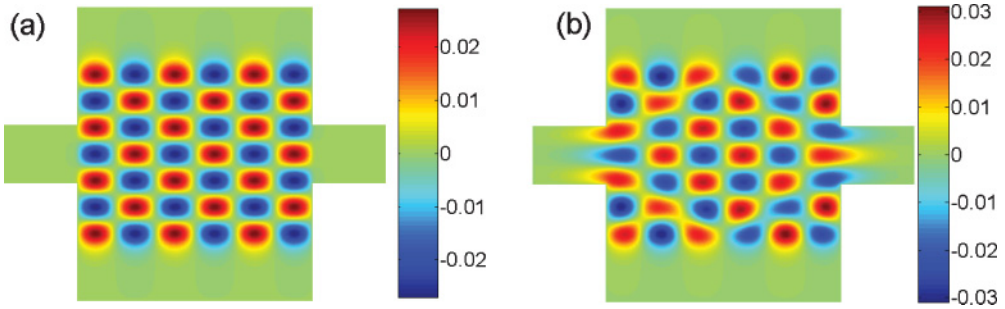

FIG. 13. (Color online) (a) Initial state is taken as the even eigenstate $\phi_{6,7}$ with eigenenergy $\epsilon_{6,7} = 7.02$. (b) Temporary state after $t = 100$. QD sizes are $L = 4, W_c = 2.9728$. This width corresponds to the second-order BSC with energy $E_c = 6.9253$.

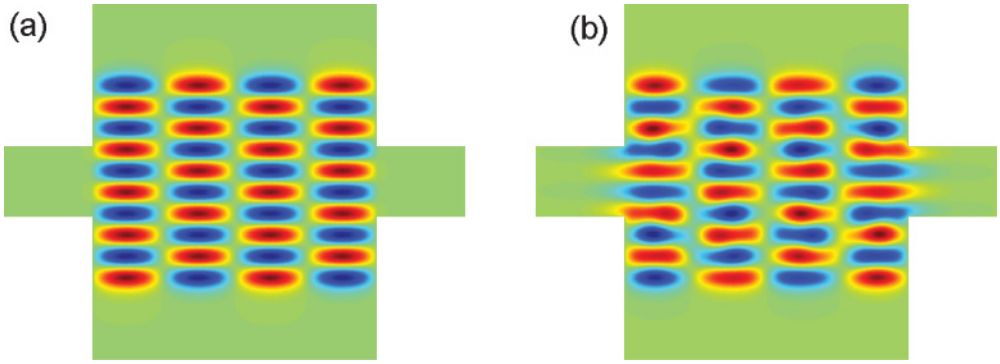

FIG. 14. (Color online) (a) Pattern of eigenstate $\phi_{4,10}$ with eigenenergy $\epsilon_{4,10} = 11.753$ that undergoes noticeable distortion upon decay to become the BSC with eigenenergy $E_c = 11.7105$ embedded into three continua $p = 1,2,3$ for $W_c = 2.9183, L = 4$ (b).

channel. Therefore, the state will decay into the first-channel continuum. However, for variation of the QD width, the state might become uncoupled with the first channel for $W = 2.9728$. Thereby we can obtain the second-order BSC. Indeed, Fig. 13 shows that, after $t = 100$, the eigenstate $\phi_{6,7}$ undergoes noticeable changes but finally is trapped in the interior of the QD. An effect of evanescent modes is substantially more profound for the BSC with high eigenenergies, as seen from Figs. 13 and 14. The strong effect of evanescent modes is seen also in Fig. 2(b).

The time evolution of the probability agrees with that result. If we took the QD's width W different from $W_c = 2.9728$ the eigenstate $\phi_{6,7}$ would decay. The closer W is to W_c the longer is the decay process.

Next, let us take the odd eigenstate $\phi_{4,10}$ with eigenenergy $\epsilon_{4,10} = 11.753$ that is uncoupled with the first-, second-, and third-channel modes for $W = 2.9183$. It also undergoes noticeable change (e.g., in energy and in wave-function pattern) to become a third-order BSC, as shown in Fig. 14.

V. CONCLUDING REMARKS

The bound state in continuum (BSC) has a similarity with the bound states below the propagation band of the continuum. They are both eigenstates of the total Hamiltonian (2), which describes the QD with leads attached. They are also both localized mainly in the QD, but have exponential tails in the leads because of coupling of the QD with the leads, and they are orthogonal to other extended eigenstates of the total Hamiltonian. The difference between them is in the positions of their discrete eigenenergies. The BSC has the energy within the propagation band of the continuum. Moreover, because of the symmetry of the QD, the BSC may be embedded simultaneously into two or three continua. We defined these BSCs as being of second or third order. As was considered in Sec. II, there might be at least four mechanisms for the BSC. The first two are similar mechanisms that are related to orthogonality of the eigenstate of the closed QD to the continuum channel mode. The third mechanism is related to the full destructive interference of at least two nearest resonance states.[38,39] Moreover, we present in Fig. 2(b) a pattern of the BSC that is the result of full destructive interference of at least three states. Finally, the Fabry-Perot mechanism is the fourth mechanism.

Irrespective of the origin of the BSC, it does not decay. This obvious result is a direct consequence of the resonance width going to zero upon approaching the BSC point (in the present case $W \to W_c$). The property of orthogonality of the BSC to the extended states of the system means that, if a plane wave is incident from the lead it has no coupling with the bound states. In other words, the bound states are "invisible" for incident waves. We can say that they are "true dark states," as was proposed by Muraguchi *et al.*[34] That statement is correct even if a quantum particle is incident in the form of a WP that is a linear superposition of the plane waves.

There is a simple way to "observe" the bound states below the continuum. One can apply a time-periodic perturbation whose frequency exceeds the distance between the bottom of propagation band and the energy of the bound state.[56] A similar approach was used in Ref. 34 where a laser field was applied to transfer the even bound state of the closed QD into the odd quasi BSC. Then the propagating wave packet is able to "see" this quasi BSC via the laser field mixing.

For the BSC we used two ways to "observe" the BSC. The first is to shrink the WD's width in time in order to reach the point of the BSC. If, for this time process, the wave packet is passing through the QD, it is able to excite the BSC, as our numerics show. Another way is the process of time decay of the proper bound states of the closed QD when at the initial time connection between the QD and leads is opened. This can be done if the gate voltage applied to quantum point contacts between the QD and the electron waveguide is decreased too fast. To use the microwave analog of the open QD[32] one can use an electrooptic shutter between the leads and microwave billiard in the case of microwave open billiards. Consideration shows that the decay processes are not simple exponential ones. For the proper choice of QD width, some eigenstates successfully evolve into true BSCs. One can use linear superposition of the eigenstates of the closed QD instead of the bare eigenstate at the initial time. This choice will yield BSCs for the time evolution. This process will be successful provided the QD width is chosen so that the equation for the BSC (9) has a solution.

[1] J. von Neumann and E. Wigner, Phys. Z. **30**, 465 (1929).
[2] F. H. Stillinger and D. R. Herrick, Phys. Rev. A **11**, 446 (1975).
[3] R. G. Newton, *Scattering Theory of Waves and Particles.* (Springer, Berlin, 1982).
[4] T. A. Weber and D. L. Pursey, Phys. Rev. A **50**, 4478 (1994).
[5] D. L. Pursey and T. A. Weber, Phys. Rev. A **52**, 3932 (1995).
[6] L. S. Cederbaum, R. S. Friedman, V. M. Ryaboy, and N. Moiseyev, Phys. Rev. Lett. **90**, 13001 (2003).
[7] H. Friedrich and D. Wintgen, Phys. Rev. A **31**, 3964 (1985).
[8] F. H. Stillinger and T. A. Weber, Phys. Rev. A **10**, 1122 (1975).
[9] D. R. Herrik, Physica B **85**, 44 (1977).
[10] F. H. Stillinger, Physica B **85**, 270 (1977).
[11] F. Capasso, C. Sirtori, J. Faist, D. L. Sivco, S.-N. G. Chu, and A. Y. Cho, Nature (London) **385**, 565 (1992).
[12] T. V. Shahbazyan and M. E. Raikh, Phys. Rev. B **49**, 17123 (1994).
[13] S. Fan, P. R. Villeneuve, J. D. Joannopoulos, M. J. Khan, C. Manolatou, and H. A. Haus, Phys. Rev. B **59**, 15882 (1999).
[14] C. Texier, J. Phys. A: Math. Gen. **35**, 3389 (2002).
[15] I. Rotter and A. F. Sadreev, Phys. Rev. E **69**, 66201 (2004); **71**, 046204 (2005).
[16] M. L. Ladrón de Guevara, F. Claro, and P. A. Orellana, Phys. Rev. B **67**, 195335 (2003).
[17] B. Wunsch and A. Chudnovskiy, Phys. Rev. B **68**, 245317 (2003).
[18] E. N. Bulgakov, K. N. Pichugin, A. F. Sadreev, and I. Rotter, JETP Lett. **84**, 508 (2006).
[19] M. L. Ladrón de Guevara and P. A. Orellana, Phys. Rev. B **73**, 205303 (2006).
[20] H. Nakamura, N. Hatano, S. Garmon, and T. Petrosky, Phys. Rev. Lett. **99**, 210404 (2007).
[21] C. S. Kim, A. M. Satanin, Y. S. Joe, and R. M. Cosby, Phys. Rev. B **60**, 10962 (1999).
[22] O. Olendski and L. Mikhailovska, Phys. Rev. B **66**, 35331 (2002).
[23] V. Vargiamidis and H. M. Polatoglou, Phys. Rev. B **72**, 195333 (2005).
[24] A. F. Sadreev, E. N. Bulgakov, and I. Rotter, Phys. Rev. B **73**, 235342 (2006).
[25] A. F. Sadreev, E. N. Bulgakov, and I. Rotter, J. Phys. A **38**, 10647 (2005).
[26] K. D. Rowe and P. J. Siemens, J. Phys. A **38**, 9821 (2005).
[27] G. Ordonez, K. Na, and S. Kim, Phys. Rev. A **73**, 022113 (2006).
[28] K.-K. Voo and C. S. Chu, Phys. Rev. B **74**, 155306 (2006).
[29] G. Cattapan and P. Lotti, Eur. Phys. J. B **60**, 51 (2007); **66**, 517 (2008).
[30] O. Valsson, C.-S. Tang, and V. Gudmundsson, Phys. Rev. B **78**, 165318 (2008).
[31] E. N. Bulgakov and A. F. Sadreev, Phys. Rev. B **78**, 075105 (2008).
[32] H.-J. Stöckmann, *Quantum Chaos: An Introduction* (Cambridge University Press, Cambridge, 1999).
[33] J. Joannopoulos, R. D. Meade, and J. Winn, *Photonic Crystals* (Princeton University Press, Princeton, 1995).
[34] M. Muraguchi, K. Shiraishi, T. Okunishi, and K. Takeda, J. Phys. Condens. Matter **21**, 064230 (2009).
[35] F. M. Dittes, Phys. Rep. **339**, 215 (2000).
[36] A. F. Sadreev and I. Rotter, J. Phys. A **36**, 11413 (2003).
[37] N. Moiseyev, Phys. Rev. Lett. **102**, 167404 (2009).
[38] A. Z. Devdariani, V. N. Ostrovsky, and Yu. N. Sebyakin, Sov. Phys. JETP **44**, 477 (1976).
[39] H. Friedrich and D. Wintgen, Phys. Rev. A **32**, 3231 (1985).
[40] V. B. Pavlov-Verevkin, Phys. Lett. A **129**, 168 (1988).
[41] A. Volya and V. Zelevinsky, Phys. Rev. C **67**, 054322 (2003).
[42] A. F. Sadreev, E. N. Bulgakov, K. N. Pichugin, I. Rotter, and T. V. Babushkina, in *Quantum Dots, Research, Technology and Applications*, edited by R. W. Knoss (Nova Sciencers Publ., Hauppauge), pp. 547–577.
[43] T. Lepetit, E. Akmansoy, J.-P. Ganne, and J.-M. Lourtioz, Phys. Rev. B **82**, 195307 (2010).
[44] M. Miyamoto, Phys. Rev. A **72**, 063405 (2005).
[45] C. S. Kim and A. M. Satanin, Phys. Rev. B **58**, 15389 (1998).
[46] E. N. Bulgakov and A. F. Sadreev, Phys. Rev. B **81**, 115128 (2010).
[47] A. F. Sadreev, E. N. Bulgakov, and I. Rotter, JETP Lett. **82**, 498 (2005).
[48] H. Lee and L. E. Reichl, Phys. Rev. B **79**, 193305 (2009).
[49] J. W. Gonzalez, M. Pacheco, L. Rosales, and P. A. Orellana, Europhys. Lett. **91**, 66001 (2010).
[50] H. Feshbach, Ann. Phys. (NY) **5**, 357 (1958); **19**, 287 (1962).
[51] J. Okołowicz, M. Płoszajczak, and I. Rotter, Phys. Rep. **374**, 271 (2003).
[52] D. V. Savin, V. V. Sokolov, and H.-J. Sommers, Phys. Rev. E **67**, 026215 (2003).
[53] S. Datta, *Electronic Transport in Mesoscopic Systems* (Cambridge University Press, 1995).
[54] E. N. Bulgakov, I. Rotter, and A. F. Sadreev, Phys. Rev. A **75**, 067401 (2007).
[55] G. B. Akguc and L. E. Reichl, Phys. Rev. E **64**, 056221 (2001); **67**, 046202 (2003).
[56] E. N. Bulgakov and A. F. Sadreev, JETP Lett. **66**, 431 (1997); JETP **87**, 1058 (1998).
[57] I. Rotter, J. Phys. A **42**, 153001 (2009).